AIAA JOURNAL
Vol. 34, No. 6, June 1996

Unsteady Pressure Loads Generated by Swept-Shock-Wave/Boundary-Layer Interactions

Sanjay Garg* and Gary S. Settles†
Pennsylvania State University, University Park, Pennsylvania 16802

An experimental research program providing basic knowledge and establishing a database on the fluctuating pressure loads produced on aerodynamic surfaces beneath three-dimensional shock-wave/boundary-layer interactions is described. A turbulent boundary layer on a flat plate is subjected to interactions with swept planar shock waves generated by sharp fins at angle of attack. Fin angles from 10 to 20 deg at freestream Mach numbers of 3 and 4 produce a variety of interaction strengths from weak to very strong. Miniature pressure transducers flush mounted in the flat plate are used to measure interaction-induced wall pressure fluctuations. The distributions of properties of the pressure fluctuations, such as their rms levels and power spectra, are determined. These are combined with and explained in light of the previously known features of the interaction flowfield. In particular, physical mechanisms responsible for the generation of high levels of surface pressure fluctuations are proposed based on the present results. Attention has been focused for the first time on the aft regions of these interactions, revealing fluctuating pressure levels as high as 155 dB. These fluctuations are dominated by low-frequency components and are caused by a previously unrecognized random motion of the primary attachment line. The maximum rms levels in the interactions show an increasing trend with increasing interaction strength. On the other hand, the maximum rms levels in the forward portion of the interactions decrease linearly with increasing interaction sweepback.

Nomenclature

A	= attachment
f	= frequency
$G(f)$	= power spectral density
L_{shock}	= length of region of intermittent separation shock translation
M	= Mach number
P	= pressure
$R(\tau)$	= cross-correlation function
S	= separation
U	= velocity
α	= angle made by fin with respect to incoming freestream direction
β	= angle made by surface flow features with respect to freestream direction, azimuth angle in spherical polar coordinates
δ	= boundary-layer thickness
δ^*	= boundary-layer displacement thickness
θ	= boundary-layer momentum thickness
σ_p	= rms (or standard deviation) of wall pressure fluctuations
τ	= time delay
ϕ, φ	= elevation angle in spherical polar coordinates

Subscripts

0	= inviscid shock location
1	= primary separation or attachment location
e	= boundary-layer edge
n	= normal to inviscid shock
S	= separation location
U	= upstream influence location
w	= wall condition
∞	= incoming freestream conditions

Received Nov. 2, 1994; revision received July 3, 1995; accepted for publication July 25, 1995.

*Research Assistant, Department of Mechanical Engineering; currently Research Scientist, High Technology Corporation, Hampton, VA 23681. Member AIAA.

†Professor, Department of Mechanical Engineering. Associate Fellow AIAA.

Introduction

MUCH effort has gone into the study of shock-wave/boundary-layer interactions (SWBLIs) over the past few decades. This class of flows, besides representing a fundamental fluid dynamics problem, is also of significant practical importance since SWBLIs are ubiquitous on the aerodynamic control surfaces and in the propulsion systems of high-speed flight vehicles. There exists a body of evidence indicating that SWBLIs are unsteady when the incoming boundary layer is turbulent, but little was known about the nature and causes of this unsteadiness until recently. Because of this inherent unsteadiness, SWBLIs can generate high-amplitude surface pressure fluctuations. These fluctuating pressure loads are especially significant in that they can occur in conjunction with high aerothermal loads and can pose a threat to the structural integrity of flight vehicles. A thorough understanding of this unsteadiness is therefore important at the vehicle design stage.

The early evidence regarding the unsteady behavior of SWBLIs was from optical results, e.g., high-speed cinema records, and was mainly qualitative. The available quantitative measurements mostly come from flush-mounted wall pressure transducers that do not disturb the flowfield. The interactions studied included those generated by forward-facing steps,[1] blunt fins,[2,3] unswept compression ramps,[4,5] etc. To date, the majority of such work has involved nominally two-dimensional flowfields. Only recently have measurements been made in swept-shock/boundary-layer interactions.[6–10] However, there are indications that many of the basic phenomenological features in swept flows are similar to those of two-dimensional interactions.

A characteristic feature observed in two-dimensional interactions is the intermittent, low-frequency, back-and-forth motion of the separation shock,[4] giving rise to a bimodal wall pressure signal near separation. The two states correspond to the undisturbed boundary-layer signature (when the shock is downstream of the transducer) and the higher pressure behind the shock (when it is upstream of the transducer). This results in a sharp rise in fluctuation intensity at separation, represented, for example, by the standard deviation of the wall pressure signal; values as large as 40 times the fluctuation level beneath the incoming boundary layer have been measured.[3]

The phenomenon of unsteady separation attracted much attention in the research community and became the almost exclusive focus of studies dealing with unsteadiness in SWBLIs. A great deal of effort was invested into understanding the dynamics of the separation

shock, as well as the physical mechanisms driving its motion. As a consequence, this phenomenon is now relatively well understood and documented, at least for two-dimensional flows. A review of the current knowledge regarding unsteady phenomena in SWBLIs involving a variety of shock generators can be found in Ref. 11.

Briefly, wall pressure measurements indicate that the large-scale, low-frequency excursions of the separation shock are caused by the expansion and contraction or trembling motion of the separation bubble, whereas the small-scale, high-frequency motion is due to fluctuations in the ratio of static quantities across the shock foot.[12] The effect of increasing interaction sweepback is a progressive decrease in the intensity of pressure fluctuations near separation coupled with an increase in the frequency range representing shock motion.[6,8–10] It is suggested by Erengil and Dolling[12] that the unsteadiness of the separation bubble in swept interactions is characterized by a trembling type, higher frequency motion as opposed to the larger scale, lower frequency expansion and contraction characteristic of two-dimensional interactions. However, no direct experimental evidence yet exists in support of this hypothesis.

One of the most commonly studied swept SWBLIs is that generated by a sharp fin at angle of attack α mounted perpendicular to a flat test surface. The fin generates a swept, planar shock wave that interacts with the zero-pressure-gradient boundary layer on the test surface. Recent studies have provided extensive knowledge about the mean surface properties[13–15] and the flowfield[16] of this sharp-fin interaction. Much of this information is summarized in the reviews by Settles and Dolling.[17,18] The most salient feature of this interaction is its quasiconical nature, which has been observed by many investigators and recently confirmed by parametric studies.[13,16,19]

The sharp-fin interaction growth is found to be essentially conical except for an initial region in the immediate vicinity of the juncture of the fin leading edge and the flat plate. The topological features of the outboard flow thus appear to emanate from a single point, which has been termed the virtual conical origin (VCO). Because of the quasiconical nature of the interaction, the most appropriate coordinate system for its study is a spherical polar system with its origin located at the VCO. Outside the initial nonconical region, the radial direction becomes degenerate (flow properties are constant along rays in a conical flow) and the flowfield can be completely described in terms of two angular dimensions: the azimuth β and the elevation ϕ.

The goal of the current study is to assess the unsteady pressure loads generated by such sharp-fin-generated swept SWBLIs and to gain a better understanding of the mechanisms involved in their generation. Also, earlier studies of these interactions have concentrated on the forward portion of the flow (near separation) while neglecting aft locations close to the fin/plate junction. In the present experiments, measurements of surface pressure fluctuations are made from front to back of the interaction, taking advantage of its quasiconical symmetry. Finally, the present study bridges the Mach number gap between the previous measurements, since it is conducted at Mach 3 and 4 for a range of interaction strengths.

Experimental Techniques

Wind-Tunnel and Test Models

The experiments were performed in the supersonic wind-tunnel facility of the Pennsylvania State University Gas Dynamics Laboratory. This wind tunnel is an intermittent blowdown type with a test section size of 15 × 17 × 60 cm and a variable Mach number capability over the range of Mach 1.5–4.0. A 55-m^3, 2000-kPa pressure reservoir provides testing times up to 2 min at stagnation pressures up to 1500 kPa.

For the present tests, a flat plate 50.8 cm long, spanning the tunnel, was mounted in the test section to provide the interaction test surface. A two-dimensional, equilibrium, nearly adiabatic, zero-pressure-gradient boundary layer forms on this plate[13] with natural transition typically occurring within 1 cm of the leading edge. A fin model with a 10-deg sharp leading edge was placed with its tip 21.6 cm from the plate leading edge and 2.62 cm from the tunnel sidewall. The fin was 12 cm long and 7.3 cm high. The height of the fin was sufficient to ensure that the interaction was semi-infinite (i.e., independent of fin height).

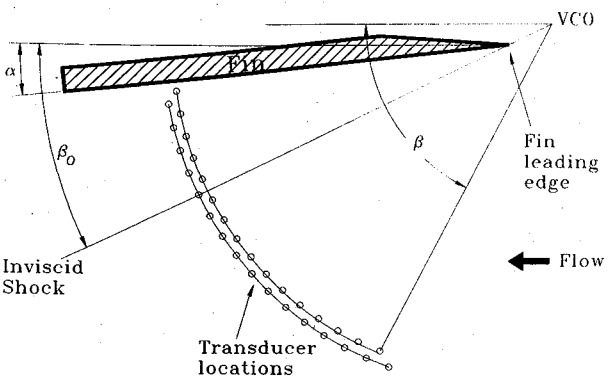

Fig. 1 Model schematic showing transducer layout.

A pneumatic fin-injection mechanism (see Ref. 13 for details) was employed to hold the fin tightly onto the flat plate and to position the fin to the desired angle of attack. Teflon tape attached to the bottom of the fin prevented leakage underneath it during the tests and also avoided metal-to-metal contact during fin motion.

A simplification afforded by the quasiconical nature of the interactions under study is that their surface properties outside the inception zone can be completely characterized by making measurements along an arc centered at the VCO. However, since the location of the VCO lies in the vicinity of the fin leading edge but varies with interaction strength, in the present experiments the measurement locations are simply arrayed along an arc centered at the fin leading edge as a first approximation. Transducer ports are provided in the flat plate at 2-deg angular separation over the range $\beta = 8$ to 70 deg with respect to the freestream direction. Figure 1 shows a schematic of the arrangement. No attempt was made to optimize transducer placement for any particular interaction. The locations of the VCO being known from previous studies,[13,16] the angular positions of the transducers were later corrected from fin leading edge to VCO. In the remainder of this article, wherever angular distributions of measured quantities are presented, this corrected (VCO-based) angle is used.

Test Conditions

The nominal Mach numbers of the present experiments were 3 and 4. The nominal stagnation chamber pressure and temperature, respectively, were 965 kPa and 300 K for Mach 3 and 1655 kPa and 300 K for Mach 4. The freestream Reynolds number was 67 × 10^6 m^{-1} and 75 × 10^6 m^{-1} for Mach 3 and 4, respectively.

Detailed pitot pressure surveys of the boundary layer at these conditions have shown that it is two dimensional and that its mean velocity profile closely matches the compressible law of the wall/law of the wake.[13] Details of the data reduction procedure can be found in Ref. 13, and only a brief description will be given here.

The measured pitot pressure profiles are converted to Mach number and then velocity profiles by assuming a constant stagnation temperature across the boundary layer. The boundary-layer edge is determined by using a 99%-freestream-velocity criterion, and the displacement and momentum thickness are calculated by numerical integration. The data are further analyzed using a method given by Sun and Childs[20] to provide the integral properties of the boundary layer such as the skin-friction coefficient and the wake strength parameter. At the location of the fin leading edge, $\delta \approx 3$, $\delta^* \approx 1.12$ and $\theta \approx 0.12$ mm. The flat plate has a negligible pressure gradient along it and is in a near-adiabatic condition.

The test cases were chosen to span a wide range of interaction strengths by varying the fin angle of attack from 10 to 20 deg at Mach 3 and from 16 to 20 deg at Mach 4. Previous investigators have found that important features of swept SWBLIs scale with the strength of the inviscid shock wave, which can be represented by the Mach number normal to the shock (M_n). The values of this parameter varied from 1.4 to 2.16 for the present cases.

Instrumentation

The pressure transducers used in the experiments are commercially available miniature devices manufactured by Kulite Semiconductor Products, Inc. (model XCQ-062-50A). They have

a pressure-sensitive area 0.071 cm in diameter and an outer case diameter of 0.163 cm. According to the manufacturer's specifications, these transducers have a natural frequency of approximately 500 kHz. However, due to the presence of a perforated screen above the transducer diaphragm, which protects it from damage due to dust particles in the flow, the frequency response is limited to about 50 kHz. The sensitivity of the transducers is typically 0.4–0.6 mV/kPa (3–4 mV/psi). These transducers were calibrated statically using a Wallace and Tiernan model 61A-1A-0100 pressure gauge.

Signal Conditioning and Data Acquisition

The pressure transducer output was amplified and low-pass filtered using Precision Filters model 6602B-I-LP1 filters (8 pole, 130 dB/octave rolloff) prior to digitization. LeCroy model 6810 Waveform Recorders with 12-bit resolution were then used to digitize and record the signals. The sampling frequency was 100 kHz and the low-pass filter cutoff frequency was 45 kHz. Six separate transducers were used in each test, their signals being simultaneously sampled and recorded. For each transducer channel, 128 records of 1024 points were acquired, yielding a total of 131,072 data points per channel per tunnel run. This sample size was large enough to ensure the convergence of its statistics. For power spectrum calculations, 128 1024-point fast Fourier transforms (FFTs) were averaged, giving a frequency resolution of 97.66 Hz.

A simple test was devised to assess the magnitude of electronic noise present in these signals. Data were acquired with the transducers exposed to a constant pressure (so that, ideally, no fluctuations were recorded), keeping the instrumentation settings the same as for the wind-tunnel tests. These data were then processed in the same fashion as actual fluctuating pressure data. This rms noise-pressure level was then compared with the rms level measured beneath the undisturbed boundary layer. The rms noise was found to be approximately one-fifth of the rms level beneath the Mach 4 boundary layer. This represents a worst case scenario, since the rms pressure beneath the Mach 3 boundary layer was twice as high due to higher static pressure, and the rms levels beneath the SWBLIs were higher still.

Results and Discussion

Incoming Boundary-Layer Measurements

The probability density distributions of the incoming boundary-layer pressure fluctuations were essentially Gaussian. The present power spectra agreed qualitatively with previously published results.[6–8] The rms of the wall pressure fluctuations normalized by the freestream dynamic pressure, σ_p/q_∞, was determined to be $2.06 \times 10^{-3} \pm 8\%$ for Mach 3 and $1.03 \times 10^{-3} \pm 9\%$ for Mach 4. These values are somewhat low compared with the semi-empirical prediction of Laganelli et al.[21] ($\sigma_p/q_\infty = 2.65 \times 10^{-3}$ and 1.85×10^{-3} for Mach 3 and 4, respectively) but agree well with the Mach 3 measurements of Tan et al.[22] ($\sigma_p/q_\infty = 2.1 \times 10^{-3}$). Experimental σ_p/q_∞ data generally tend to fall below the actual values due to the finite size of the transducers used, which are large compared with the length scales of the fine-scale turbulent structures in the boundary layer, thus tending to eliminate the contributions of high-frequency fluctuations. The incoming boundary layer also has significant energy above the filter cutoff frequency (about 45 kHz), since a typical large eddy frequency in the present experiments is 200 kHz (U_e/δ). However, since the pressure fluctuations in the SWBLIs are dominated by relatively low frequencies, this is not considered to be a serious limitation.

Interaction Measurements

RMS Distributions

Distributions of the rms pressure fluctuation level, σ_p, along with the corresponding mean pressure distributions are presented in Fig. 2 for example interactions at $M_\infty = 3$ and 4 and $\alpha = 20$ deg. These rms values are shown twice, being normalized by both the freestream pressure P_∞ and the local mean pressure P_w. An error analysis indicates that the combined random error due to all sources (electronic noise, calibration uncertainty, tunnel vibration, temperature drift, etc.) is ±5% in these measurements. Note that this estimate does not include the bias error caused by inadequate transducer resolution, which is discussed later. A determination of this bias requires knowledge of the scales of pressure-producing structures through the interaction and has not been attempted here.

The flowfield maps constructed by Alvi and Settles[16] for these cases are also shown in Fig. 2. Note that the flowfield maps are drawn to the same β scale as the rms and mean pressure distributions, facilitating visual comparison of the three. Some features are indicated by vertical reference lines for ease of comparison with the flowfield maps. The locations of surface flow features (such as primary separation and attachment) in the flowfield maps are determined from surface flow visualization[13,16] and only known within ±2 deg.

The rms pressure distributions display features that are apparently universal in SWBLIs—both two and three dimensional. One of these is the peak observed near primary boundary-layer separation S_1. It is generally agreed that this sharp increase in rms pressure levels above the incoming boundary-layer level is caused by the intermittent back-and-forth motion of the separation shock in a region bounded by the upstream influence and mean separation lines. In two-dimensional interactions, the magnitude of this peak is much larger (as much as 40% of the local mean pressure) than in the present swept interactions. Its low present value (0.039 max) suggests that intermittency is less pronounced in swept interactions. However, the values measured by Tran[6] in swept interactions with the same Mach number and fin angle were almost twice as high.

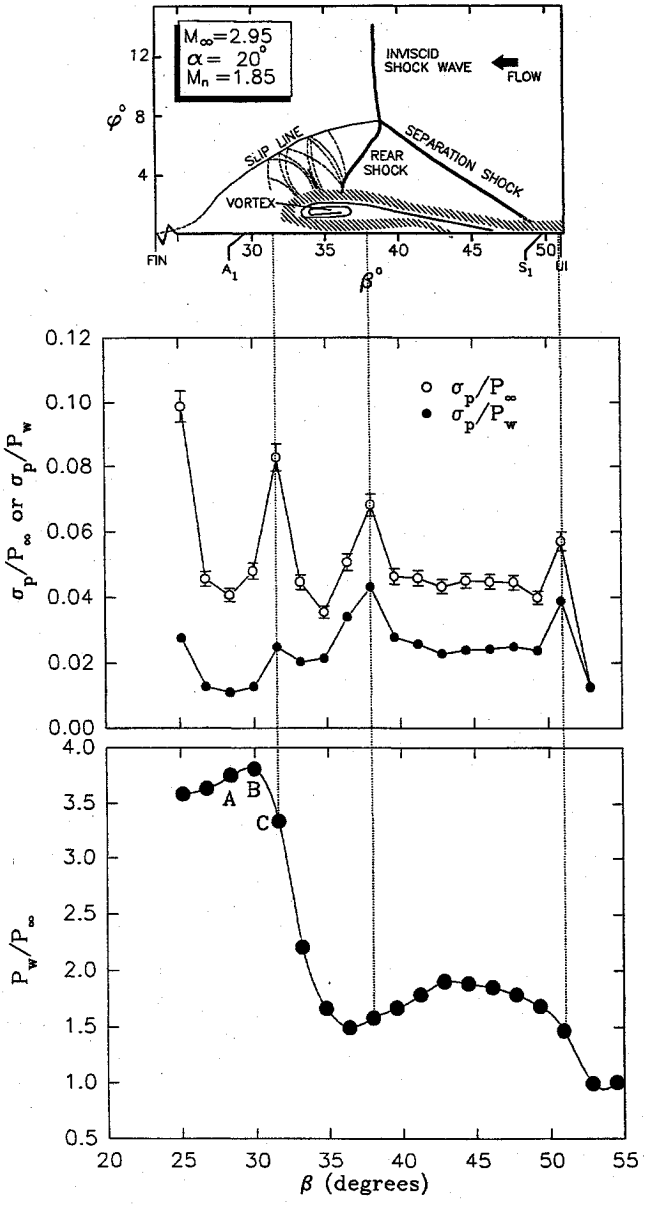

Fig. 2a Flowfield map, rms pressure distribution, and mean pressure distribution for $M_\infty = 3$ and $\alpha = 20$ deg.

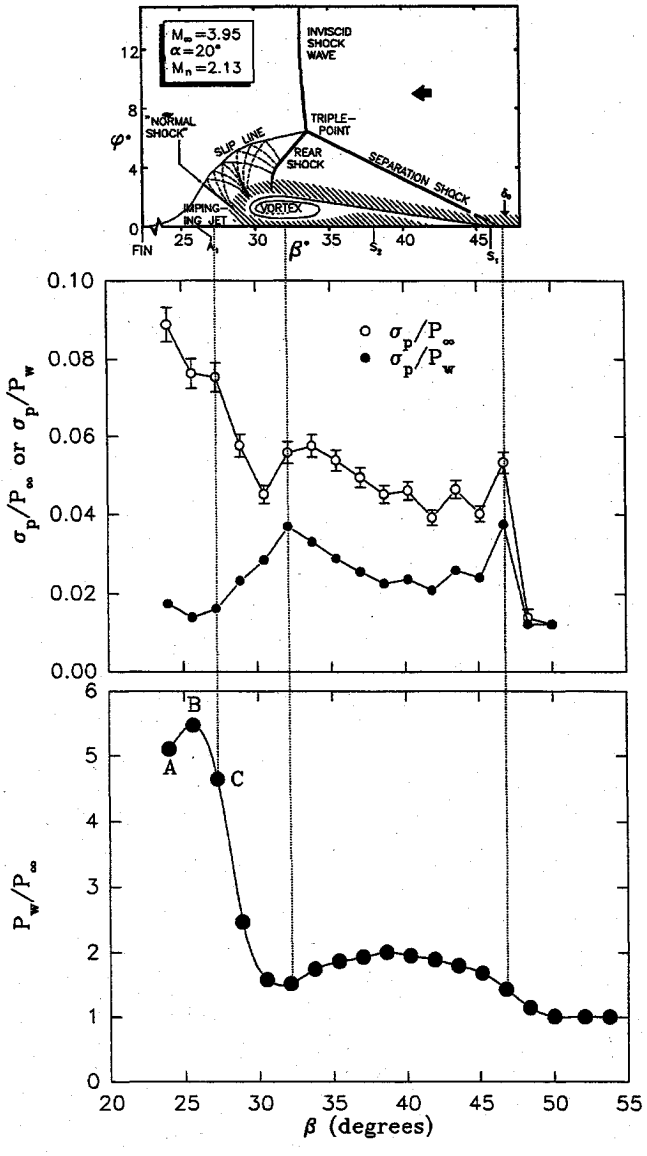

Fig. 2b Flowfield map, rms pressure distribution, and mean pressure distribution for $M_\infty = 4$ and $\alpha = 20$ deg.

The comparatively low values measured in this study are probably due to spatial resolution limitations of the present measurements as discussed later.

A striking feature of the wall pressure signals recorded in the present tests is that the fluctuations near primary separation do not exhibit any of the characteristics of intermittent separation. It has been noted by many investigators that the probability density function (PDF) of an intermittent signal is distinctly non-Gaussian, usually being highly skewed or bimodal. In the present study—for all of the cases tested—the PDFs were found to be essentially Gaussian throughout the so-called intermittent region. Even close visual inspection of the raw pressure time histories did not reveal any evidence of intermittency in the present data. Similar results have been reported by Gibson and Dolling[7] from their study of sharp-fin-generated interactions at Mach 5.

The cause of this discrepancy lies in the limited spatial resolution problem of the present measurements and those of Gibson and Dolling.[7] Both sets of experiments were conducted beneath relatively thin flat plate boundary layers, whereas previous experiments[6] had utilized wind-tunnel floor boundary layers that were approximately an order of magnitude thicker.

In the present study, the boundary-layer thickness is only twice the transducer diameter, and the spacing between adjacent transducers is approximately equal to the boundary-layer thickness. Since the typical length scale of the region within which the separation shock translates intermittently (called L_{shock} by some investigators) is of the same order of magnitude as the boundary-layer thickness (e.g., see Dolling and Or[5]), it is probable that this region either falls between two adjacent transducers or else completely upon the face of one transducer when the boundary layer is thin. In either case, the pressure signal thus recorded, due to averaging, will not reveal intermittency even if it is present. This explanation was confirmed by the experiments of Schmisseur and Dolling,[8] who carried out tests in the same facility and at the same conditions as did Gibson and Dolling,[7] except that a much thicker tunnel wall boundary layer was used. The results revealed that intermittent separation was indeed present in thick-boundary-layer interactions and the characteristics of the wall pressure fluctuations near separation were similar to those observed by earlier researchers, given sufficient transducer resolution to detect them.

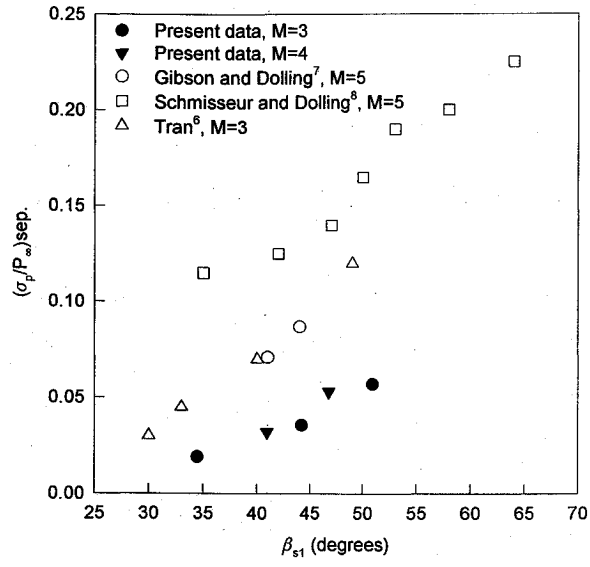

Fig. 3 Maximum rms near separation as a function of separation line angle.

Figure 3 shows a plot of the normalized magnitude of the fluctuating pressure peak near primary separation vs the angle of the primary separation line β_{s1}. Data from the other three sharp-fin studies[6–8] are also included for comparison. All four data sets display an approximately linear increase in $(\sigma_p/P_\infty)_{\text{sep}}$ with increasing β_{s1}. The greater the separation line angle (i.e., the less sweptback the interaction), the higher the fluctuation intensity. Thus interaction sweepback may be employed to ameliorate the pressure loads due to unsteady separation in SWBLIs.

Also, it is evident that separation line angle alone is not sufficient to correlate data from different experiments. Some of the variations may be caused by differences in the ratio of boundary-layer thickness to transducer diameter among these studies. Figure 3 shows that, at the same Mach number (present Mach 3 data, Tran's data, and Mach 5 data of Refs. 7 and 8), the experiment with the thicker boundary layer exhibits larger fluctuations at separation. As explained earlier, it is possible that the thin boundary-layer studies lack the resolution necessary to faithfully record the intermittent motion of the separation shock and thus underestimate the magnitude of the fluctuating pressure peak in this region.

Aft of the separation peak, the rms level in Fig. 2 is observed to drop and remain relatively constant for some angular distance. This region approximately corresponds to the so-called plateau region in the mean pressure distributions. Examination of the flowfield maps reveals that there are no significant changes in the flowfield (both on and off the surface) over much of this region.

The next feature in the rms distributions of Fig. 2 is the appearance of a second peak in the vicinity of the dip in the mean pressure distribution. The magnitude of this peak (when normalized by the local mean pressure) is approximately the same as that of the peak associated with separation. It can be seen that this downstream fluctuating pressure peak lies close to the core of the separation vortex. This peak is observed in all of the present test cases as well as in the experiments reported in Ref. 8.

It is believed that this local maximum in the distributions of rms pressure levels is caused by the separation vortex core. The data do not allow identification of the exact mechanism responsible, but it may be the result of a general unsteadiness of the vortex itself. Note that the mean static pressure P_w/P_∞ changes rapidly on either side of this peak (especially aft of it). A fluctuation in the position of the vortex core and its associated mean pressure distribution could cause high levels of fluctuating loads to be generated. Richards and Fahy[23] have reported the existence of a similar peak in pressure fluctuation levels beneath the core of the separated vortex on the upper surface of delta wings at incidence.

Further downstream, the rms pressure level reaches yet another maximum near the primary attachment line A_1 in the impinging-jet region of the flowfield. For all of the cases tested, the absolute magnitude of this local maximum is larger than either of the other two peak values described earlier. This feature of the rms pressure distributions has been clearly observed for the first time in the present study. Discussion of the possible physical mechanism responsible for its generation will be deferred until after the power spectra of pressure fluctuations are presented below. It should be noted that this peak is more readily discernible in the Mach 3 case (Fig. 2a) than in the Mach 4 interaction (Fig. 2b). This is because the higher Mach number case is more highly swept, and hence the attachment line is pushed closer to the fin. Indeed, in the $M_\infty = 4$ and $\alpha = 20$ deg interaction of Fig. 2b, this peak merges with the high rms pressure levels near the fin/plate junction and there exists no valley in the rms distribution between them.

Finally, the rms pressure levels are observed to rise again as the fin/plate junction is approached. For the interactions presented, the highest rms level is observed at the location closest to the fin/plate junction. The highest fluctuating pressure level recorded in the present experiments is roughly 10% of the freestream static pressure in the $M_\infty = 3$ and $\alpha = 20$ deg case. Scaled to an altitude of 50,000 ft where $P_\infty = 11650$ Pa (1.69 psi), this rms value represents

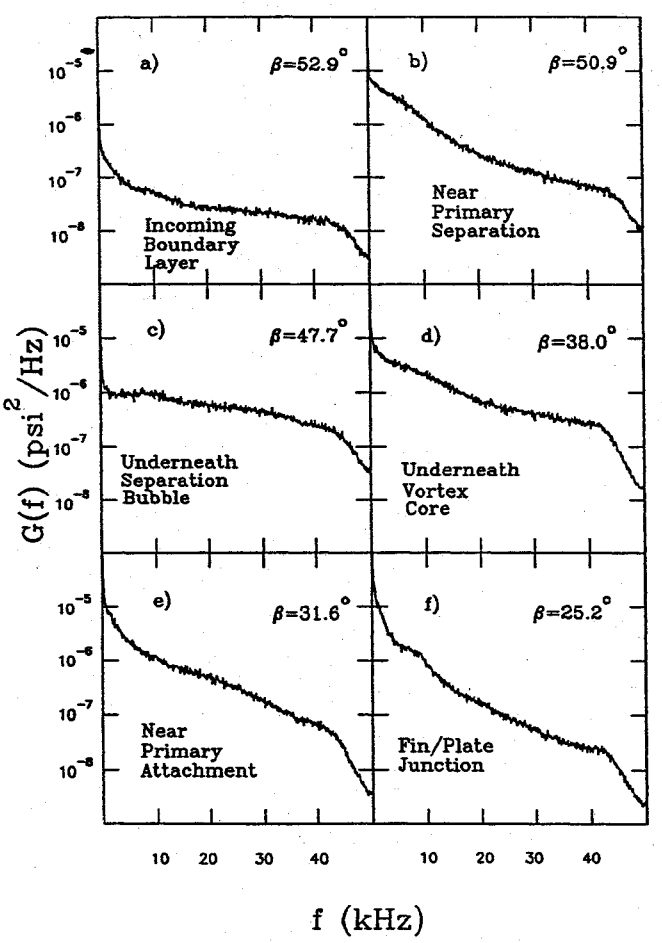

Fig. 4 Power spectra of wall pressure fluctuations for $M_\infty = 3$ and $\alpha = 20$ deg interaction.

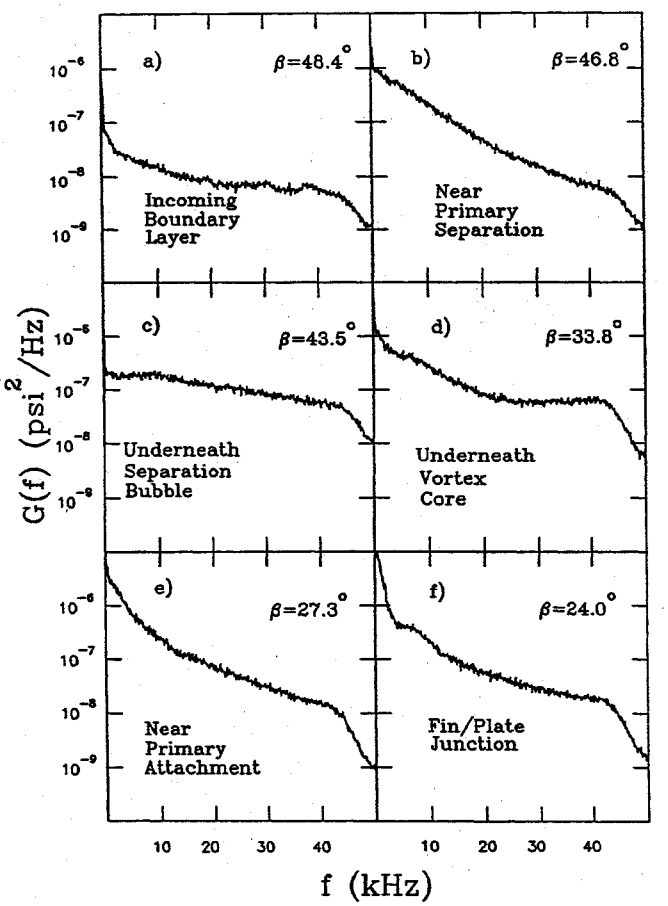

Fig. 5 Power spectra of wall pressure fluctuations for $M_\infty = 4$ and $\alpha = 20$ deg interaction.

a sound pressure level of 155 dB (referenced to 20 μPa absolute). This places the present interactions in the category of significant and possibly dangerous unsteady pressure-load generators.

Power Spectra of Pressure Fluctuations

Figures 4 and 5 present the power spectra from the present Mach 3 and 4, $\alpha = 20$ deg interactions at locations ranging from the undisturbed boundary layer to the fin/plate junction. These spectra are representative of the trends observed in all of the other interaction cases studied. The corresponding flowfield maps can be seen in Fig. 2. The abscissa of Figs. 4 and 5 is the raw power spectral density (PSD) plotted on a logarithmic scale. (The conventional practice of normalizing the PSD by the rms level has deliberately not been followed here to show more clearly the evolution of the energy content of different frequency ranges through the interaction.)

As expected, the incoming boundary-layer spectra are broadband and approximately flat up to the filter cutoff frequency of about 45 kHz. Note that there is significant energy above the cutoff, as mentioned earlier. However, since the present focus of interest is on the higher amplitude, lower frequency fluctuations in the interaction, this is not a serious limitation.

Near primary separation (Figs. 4b and 5b), a dramatic increase in energy up to about 30 kHz is observed. This is thought to be due to the motion of the separation shock. No coherent shock-motion frequencies are evident; however, the increased energy is spread over a wide range of frequencies. Further downstream, under the separation bubble, the spectrum relaxes back to its original shape, but with increased energy content over the entire range of frequencies measured (Figs. 4c and 5c). This is reflected in the elevated rms levels also seen at these locations (see Fig. 2). Referring to the flowfield maps in Fig. 2, one sees no new flow features for some angular distance downstream of primary separation, and the spectrum shape remains approximately the same in this region.

Then, as the location of the vortex core is approached (Figs. 4d and 5d), an increase in energy is observed in the frequency range 0–20 kHz. This is followed by an increase of energy at low frequencies

and a simultaneous decrease in the strength of high-frequency fluctuations at locations still further aft. This is likely because such aft locations are relatively isolated from the influence of the turbulent separated shear layer, which wraps around the vortex core and becomes a part of the reverse flow upstream of these locations (see the flowfield maps in Fig. 2). At the rms peak in the impinging jet region (Figs. 4e and 5e), the shape of the spectrum is similar to that recorded at the peak near separation.

The spectra closest to the fin/plate junction, where the highest rms levels were measured, are dominated by very low frequencies in the range 0–5 kHz (Figs. 4f and 5f). It is possible that this is due to the flapping motion of the slip line, which was observed by Alvi and Settles.[16]

Unsteady Attachment

It is believed that the high fluctuating pressure levels near the primary attachment line A_1 are caused by a random fluctuation in the instantaneous position of the attachment line. Note that the attachment line location is approximately coincident with the location of the peak in the mean pressure distribution. Conceptually, such a motion of the attachment line may be equated to movement of the mean pressure distribution back and forth over a transducer at a fixed location. Since there exist large mean pressure gradients in the vicinity of the reattachment line, such a motion will cause high fluctuating pressure levels to be generated. Further, since the mean pressure gradient is much higher upstream of the mean pressure peak than aft of it (see Fig. 2), the peak in rms pressure level occurs immediately upstream of the peak in the mean pressure distribution.

The line of reasoning outlined earlier was prompted by the work of Kuethe et al.,[24,25] who made measurements of velocity fluctuations in the vicinity of the stagnation points on blunt bodies in a uniform flow. These were found to be significantly higher than those in the freestream, the increased energy being composed mainly of low-frequency fluctuations. The authors postulated that this was due to a random motion of the stagnation point. The correlation between simultaneously recorded velocity fluctuations on opposite sides of the mean stagnation point had a large negative value at zero time delay. This indicated that, if at any instant the instantaneous velocity on one side of the stagnation point was higher than the mean value at that location, then the instantaneous velocity on the opposite side of the stagnation point was correspondingly lower than the mean and vice versa. This was found to be the case for subsonic as well as supersonic flow and constituted strong evidence in support of the authors' hypothesis. Kuethe et al.[24,25] further found that if the model geometry was changed such that the stagnation point became fixed, the velocity fluctuations in its vicinity fell to a very low value.

A two-point analysis similar to that of Kuethe et al. described earlier was carried out with the present data. The locations of interest are labeled A, B, and C on the mean pressure distributions of Fig. 2. Locations A and C lie on opposite sides of the mean pressure peak, whereas location B is approximately coincident with it.

Figure 6 shows the space–time correlation, as a function of time delay, between the pressure signals from locations A and B and locations A and C for the two interactions. The quantity of interest is the value of the correlation at zero time delay. It can be seen that this is a large positive value for locations A and B (which are in close proximity to one another) and a large negative value for locations A and C. (By definition, the space–time correlation between two random signals must lie within the range -1 to $+1$.) This indicates that, on average, when the pressure at location A is higher than the mean, so is that at location B and vice versa. For locations A and C, the trends are the opposite, viz., when the pressure at A rises, that at C falls, and vice versa. (The cross correlation for the $M_\infty = 3$ case in Fig. 6a seems to level off at a constant value of 0.4 at large time delays. At first glance, this behavior is somewhat surprising; however, an explanation was found by examination of the time history of pressure fluctuations. These contain disturbances of the order of a few hertz in frequency, which will cause high correlations for time delays as large as several hundred milliseconds. Why similar fluctuations are not observed in the $M_\infty = 4$ case is unclear.)

This observation is consistent with the view that the mean pressure distribution translates back and forth in the vicinity of the attachment line, giving rise to high levels of fluctuating pressure loads. Considering the shape of the mean pressure distribution in the vicinity of the attachment line, it is clear that a shift of the curve in either direction would cause simultaneous pressure changes of opposite sign at fixed locations on opposite sides of the peak (locations A and C). It should be noted that the instantaneous pressure distribution is probably sharper than the mean pressure distribution, which is smeared out in comparison. The instantaneous pressure distribution has sharper crests and troughs and steeper gradients than the mean pressure curve, which would accentuate the pressure fluctuations caused by shifts in its position.

This behavior can be more easily visualized by an examination of Fig. 7, which shows an example of simultaneously sampled time histories from the pressure signals at the locations being considered. It can be seen that the pressure signals from locations A and B change in concert with one another, whereas those at locations A and C follow the opposite trends, almost to the extent of mirror imaging. A

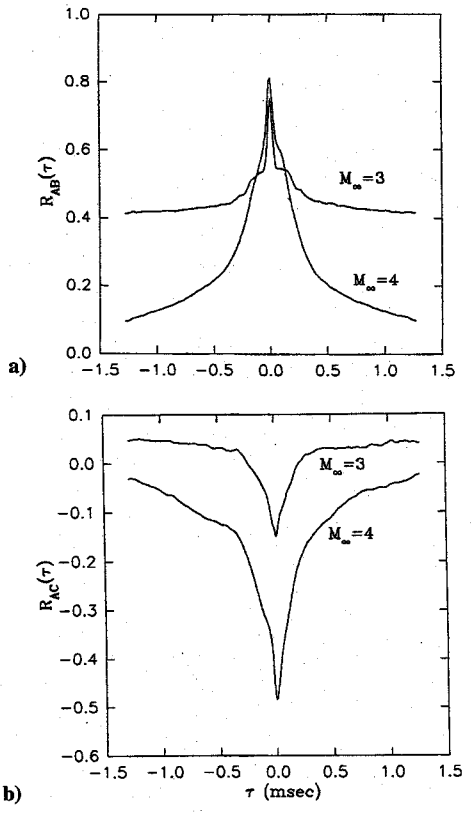

Fig. 6 Space–time correlation functions for locations near the primary attachment line: a) locations A and B in Fig 2 and b) locations A and C in Fig. 2.

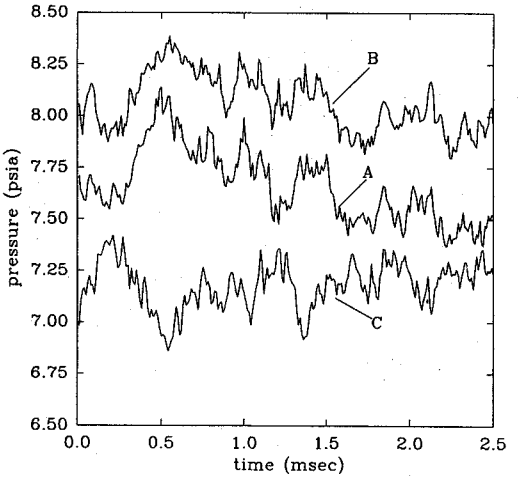

Fig. 7 Simultaneous time traces from locations A, B, and C from the $M_\infty = 4$ and $\alpha = 20$ deg interaction.

further observation from Fig. 7 is that only relatively low-frequency fluctuations behave in this manner; high-frequency changes in the pressure signals do not necessarily follow the same trends. In fact, these seem to be uncorrelated for the signals being considered.

Having determined that random movement of the attachment line and the associated mean pressure distribution is the physical mechanism responsible for high levels of pressure fluctuations near the attachment line in the present interactions, the question may be posed: What, in turn, causes this movement of the attachment line? A definitive answer to this query is not possible at present; however, some hypotheses can be advanced.

The attachment stream surface originates in the freestream flow and lies close to the boundary-layer edge.[16,26] It passes through the separation shock close to its foot, is turned upward, and then is turned back toward the surface of the plate by the rear shock, finally becoming part of the impinging jet. It is therefore possible that the intermittent motion of the separation shock transmits fluctuations to the attachment location. A change in the position or angle of the separation shock can change the flow properties in a streamtube containing the attachment stream surface and result in a displacement of the instantaneous attachment location. The power spectra of pressure fluctuations shown in Figs. 4 and 5 lend some support to this view. Similar spectral behavior is observed for locations at primary separation and at the rms pressure peak near attachment (compare Figs. 4b and 4e and Figs. 5b and 5e). Thus, it is suggested that the motion of the attachment line is intimately related to the much-studied unsteadiness of the separation shock itself.

This hypothesis is supported by the findings of Gramann and Dolling,[27] who made simultaneous wall pressure measurements underneath the separation shock and near the reattachment location in a two-dimensional compression corner interaction. They observed that the separation bubble expands and contracts, at the same frequencies as the separation shock motion. Further work by Gramann and Dolling[28] revealed that the large-amplitude, low-frequency component of the pressure signals near reattachment correlated with the motion of the separation shock. They concluded that the mean pressure distribution translated back and forth on the ramp face due to the motion of the separation shock. It was further noted that the major contribution to the overall rms pressure level on the ramp surface (near reattachment) came from this motion of the mean pressure distribution. These observations led the authors to characterize the flowfield on the ramp surface as a frozen flowfield that translated upstream and downstream with the reattachment point, much as in the model proposed earlier for fin interactions near the attachment line.

In the present experiments, simultaneous wall pressure measurements beneath the foot of the separation shock and near the attachment line were not made. It was therefore not possible to apply the techniques used by Gramann and Dolling and further test our hypothesis concerning the connection between the unsteadiness of the separation shock and the high rms pressure levels observed near attachment. Nonetheless, it is the view of the authors that there exist sufficient similarities between the two cases to justify an extrapolation of the conclusions of Gramann and Dolling[27,28] to the present work.

A further similarity between the behavior near separation and attachment is the shape of the mean pressure distribution at the local rms pressure peak. In both cases, the maximum in rms pressure appears to be coincident with the point where the mean pressure gradient is largest (these points are also points of inflection of the mean pressure distribution). A simple explanation for this behavior is as follows: for small displacements of the pressure distribution, the pressure change caused would be proportional to the product of pressure gradient and displacement magnitude. Thus the rms pressure peak would coincide with the location of maximum absolute mean pressure gradient.

Conclusions

Fluctuating pressure measurements have been made beneath swept SWBLIs generated by sharp fins at angles of attack between 10 and 20 deg at Mach 3 and 4. The interactions thus generated ranged from weak, barely separated, to strong, well-separated flowfields. Measurements were made across the entire range from front to back of these interactions. Analysis of the data provided distributions of the rms pressure fluctuations and their spectral content. The conclusions reached can be summarized as follows.

1) The class of interactions under study can generate significant fluctuating pressure loads on portions of high-speed aircraft. The highest loads are experienced at locations closest to the foot of the fin that generates the swept shock wave. These are dominated by low-frequency fluctuations in the range 0–5 kHz and reach a maximum sound pressure level of 155 dB in the cases studied.

2) The phenomenon of intermittent separation, that has attracted much attention in two-dimensional interactions, is less significant in swept interactions. An rms pressure peak associated with motion of the separation shock is observed in the current experiments. However, the magnitude of this peak decreases with increasing sweepback of the separation line.

3) Spatial resolution of the transducers employed can have a significant influence upon the detection of intermittent separation in these interactions. Transducers of a size comparable to the extent of shock motion are unable to detect intermittency, resulting in underestimated rms pressure levels and erroneous probability density functions near separation. This was the case in the current experiments.

The pressure fluctuations felt at the wall are undoubtedly intimately related to the behavior of the flowfield off the surface. Thus it is important to attempt to explain the observed behavior of surface pressure fluctuations in light of the known features of the off-surface flow. Previous studies have focused almost exclusively on the unsteady separation shock wave as a pressure fluctuation generation mechanism. The present work has identified additional flowfield features that are believed to be responsible for high levels of fluctuating pressure loads in the interactions.

1) The core of the separation vortex is one mechanism responsible for the generation of high fluctuating pressure loads in these interactions.

2) A peak in the rms pressure distribution in the vicinity of the mean attachment line was clearly observed for the first time in the present study. The mechanism responsible for this peak is a random fluctuation in the instantaneous location of the attachment line. This generates high rms pressure levels through the translation of the mean pressure distribution in this region.

3) The available evidence suggests that this phenomenon is closely coupled to the unsteadiness of the separation shock. It is possible that these two phenomena share a common cause, such as the trembling motion of the separation bubble suggested by Erengil and Dolling.[12]

4) The junction of the fin and the flat plate is yet another location where high fluctuating pressure loads are felt. These appear to be caused by the unsteadiness of the slip line, as observed by earlier investigators.

5) The principal mechanism of unsteady surface pressure load generation in swept SWBLIs appears to be the unsteady motion of inflection points (or points of largest gradient) in the mean pressure distribution.

Acknowledgments

This work was supported by NASA Langley Grant NAG 1-1070, monitored by William Zorumski.

References

[1]Kistler, A. L., "Fluctuating Wall Pressure Under a Separated Supersonic Flow," *Journal of the Acoustical Society of America*, Vol. 36, March 1964, pp. 543–550.

[2]Degrez, G., "Exploratory Experimental Investigation of the Unsteady Aspects of Blunt Fin-Induced Shock Wave Turbulent Boundary Layer Interactions," M.S.E. Thesis, Mechanical and Aerospace Engineering Dept., Princeton Univ., Princeton, NJ, June 1981.

[3]Dolling, D. S., and Bogdonoff, S. M., "An Experimental Investigation of the Unsteady Behavior of Blunt Fin-Induced Shock Wave Turbulent Boundary Layer Interactions," AIAA Paper 81-1287, June 1981.

[4]Dolling, D. S., and Murphy, M. T., "Unsteadiness of the Separation Shock Wave Structure in a Supersonic Compression Ramp Flowfield," *AIAA Journal*, Vol. 21, No. 12, 1983, pp. 1628–1634.

[5]Dolling, D. S., and Or, C. T., "Unsteadiness of the Shock Wave Structure in Attached and Separated Compression Ramp Flowfields," *Experiments in Fluids*, Vol. 3, No. 1, 1985, pp. 24–32.

[6]Tran, T. T., "An Experimental Investigation of Unsteadiness in Swept Shock Wave/Boundary Layer Interactions," Ph.D. Dissertation, Mechanical and Aerospace Engineering Dept., Princeton Univ., Princeton, NJ, March 1987.

[7]Gibson, B., and Dolling, D. S., "Wall Pressure Fluctuations Near Separation in a Mach 5, Sharp Fin-Induced Turbulent Interaction," AIAA Paper 91-0646, Jan. 1991.

[8]Schmisseur, J. D., and Dolling, D. S., "Unsteady Separation in Sharp Fin-Induced Shock Wave/Turbulent Boundary Layer Interaction at Mach 5," AIAA Paper 92-0748, Jan. 1992.

[9]Garg, S., and Settles, G. S., "Wall Pressure Fluctuations Beneath Swept Shock/Boundary Layer Interactions," AIAA Paper 93-0384, Jan. 1993.

[10]Erengil, M. E., and Dolling, D. S., "Effects of Sweepback on Unsteady Separation in Mach 5 Compression Ramp Interactions," *AIAA Journal*, Vol. 31, No. 2, 1993, pp. 302–311.

[11]Dolling, D. S., "Fluctuating Loads in Shock Wave/Turbulent Boundary Layer Interaction: Tutorial and Update," AIAA Paper 93-0284, Jan. 1993.

[12]Erengil, M. E., and Dolling, D. S., "Physical Causes of Separation Shock Unsteadiness in Shock Wave/Turbulent Boundary-Layer Interactions," AIAA Paper 93-3134, July 1993.

[13]Lu, F. K., "Fin Generated Shock-Wave Boundary-Layer Interactions," Ph.D. Dissertation, Mechanical Engineering Dept., Pennsylvania State Univ., University Park, PA, Feb. 1988.

[14]Kim, K. S., "Skin Friction Measurements by Laser Interferometry in Supersonic Flows," Ph.D. Dissertation, Mechanical Engineering Dept., Pennsylvania State Univ., University Park, PA, Dec. 1988.

[15]Lee, Y., "Heat Transfer Measurements in Swept Shock Wave/Turbulent Boundary-Layer Interactions," Ph.D. Dissertation, Mechanical Engineering Dept., Pennsylvania State Univ., University Park, PA, June 1992.

[16]Alvi, F. S., and Settles, G. S., "Physical Model of the Swept Shock Wave/Boundary-Layer Interaction Flowfield," *AIAA Journal*, Vol. 30, No. 9, 1992, pp. 2252–2258.

[17]Settles, G. S., and Dolling, D. S., "Swept Shock Wave/Boundary-Layer Interactions," *Tactical Missile Aerodynamics*, edited by M. Hemsch and J. Nielsen, Vol. 104, Progress in Astronautics and Aeronautics, AIAA, New York, 1986, pp. 297–379.

[18]Settles, G. S., and Dolling, D. S., "Swept Shock Wave/Boundary-Layer Interactions—Tutorial and Update," AIAA Paper 90-0375, Jan. 1990.

[19]Zheltovodov, A. A., Maksimov, A. I., and Shilein, E. K., "Development of Turbulent Separated Flows in the Vicinity of Swept Shock Waves," *The Interactions of Complex 3-D Flows*, edited by A. M. Kharitonov, Akademia Nauk USSR, Inst. of Theoretical and Applied Mechanics, Novosibirsk, 1987, pp. 67–91.

[20]Sun, C. C., and Childs, M. E., "A Modified Wall-Wake Velocity Profile for Turbulent Compressible Boundary Layers," *Journal of Aircraft*, Vol. 10, No. 6, 1973, pp. 381–383.

[21]Laganelli, A. L., Martelluci, A., and Shaw, L. L., "Wall Pressure Fluctuations in Attached Boundary Layer Flow," *AIAA Journal*, Vol. 21, No. 4, 1983, pp. 495–502.

[22]Tan, D. K. M., Tran, T. T., and Bogdonoff, S. M., "Surface Pressure Fluctuations in a Three-Dimensional Shock Wave/Turbulent Boundary Layer Interaction," AIAA Paper 85-0125, Jan. 1985.

[23]Richards, E. J., and Fahy, F. J., "Turbulent Boundary Layer Pressure Fluctuations over Two-Dimensional Surfaces and Narrow Delta Wings," *Acoustical Fatigue in Aerospace Structures, Proceedings of the Second International Conference* (Dayton, OH), edited by W. J. Trapp and D. M. Forney Jr., Syracuse Univ. Press, Syracuse, NY, 1965, pp. 39–62.

[24]Kuethe, A. M., Willmarth, W. W., and Crocker, G. H., "Stagnation Point Fluctuations on a Body of Revolution," *Physics of Fluids*, Vol. 2, No. 6, 1959, pp. 714–716.

[25]Kuethe, A. M., Willmarth, W. W., and Crocker, G. H., "Turbulence Field near the Stagnation Point on Blunt Bodies of Revolution," *Proceedings of the 1961 Heat Transfer and Fluid Mechanics Institute*, edited by R. C. Binder, M. Epstein, R. L. Mannes, and H. T. Yang, Stanford Univ. Press, Stanford, CA, 1961, pp. 10–22.

[26]Knight, D. D., and Badekas, D., "On the Quasi-Conical Flowfield Structure of the Swept Shock Wave-Turbulent Boundary Layer Interaction," AIAA Paper 91-1759, June 1991.

[27]Gramann, R. A., and Dolling, D. S., "Dynamics of Separation and Reattachment in a Mach 5 Unswept Compression Ramp Flow," AIAA Paper 90-0380, Jan. 1990.

[28]Gramann, R. A., and Dolling, D. S., "Dynamics of the Outgoing Turbulent Boundary Layer in a Mach 5 Compression Ramp Interaction," AIAA Paper 90-1645, June 1990.